Advances in Theory of Photonic Crystals

Shanhui Fan, *Senior Member, IEEE*, Mehmet Fatih Yanik, Zheng Wang, *Student Member, IEEE*, Sunil Sandhu, and Michelle L. Povinelli

Invited Paper

***Abstract*—In this paper, the authors review some of the recent advances in the theory of photonic crystals, drawing examples from their own work in magnetooptical and dynamic photonic crystals. The combination of theory and simulations shows that these crystal structures exhibit rich optical physics effects and can provide new ways to accomplish sophisticated optical information-processing tasks.**

***Index Terms*—Dynamic photonic crystals, magneto-optical effects, photonic crystals, stopped light, time-reversal of light.**

I. Introduction

SINCE the pioneering works by Yablonovitch [1] and John [2], the properties of photonic crystals have been intensively studied for the past 20 years. Many important predicted properties, including, for instance, the existence of the complete photonic band gap [1], [2], the control of spontaneous emission [1], and the construction of ultracompact light wave circuits [3], have by now been experimentally demonstrated. The band structures of perfect crystals, as well as the properties of the defect states, have also been studied in great detail and reviewed in articles and books [4]–[8]. Recent research works have therefore focused on functionalizing photonic crystal structures to exploit their remarkable properties to control even wider ranges of active, nonlinear, and dynamic optical properties.

In this context, here, we provide a brief review of some of our own recent research activities aiming to advance the theory of photonic crystals. The examples chosen here include magnetooptical photonic crystals, considered in Section II, which are important for on-chip signal isolation [9]–[11] and dynamic photonic crystals, discussed in Section III, which open the possibility for coherent optical pulse stopping and storage [12]–[17]. In both cases, the use of photonic crystals provides a path toward accomplishing crucial optical information-processing tasks that are very difficult to achieve with conventional means. Also, in each case, the use of photonic crystals leads to important new optical physics effects. In the case of magnetooptics, we show that time-reversal symmetry breaking in photonic crystal provides a fundamental protection against the effect of disorder. Similarly, dynamic processes in photonic crystal allow one to mold the spectrum of a photon pulse almost at will while completely preserving coherent information in the optical domain. Thus, from both the fundamental physics and device application points of view, there is still a great deal that can be accomplished in theoretical studies of photonic crystals.

Earlier theoretical studies of photonic crystals have focused on elucidation of the band diagrams and the modal properties of passive dielectric photonic crystal systems. Here, we note that, based on this knowledge, it is then possible to construct analytic models with only a few dynamic variables, which are nevertheless capable of describing complex optical processes in photonic crystals in detail. The developments of analytic theory will prove to be increasingly important as we try to discover more remarkable properties in photonic crystals, as well as in the model abstraction that is important for analysis and synthesis of device functions.

II. Magnetooptical Photonic Crystals

One of the most fundamental challenges to the creation of on-chip large-scale integrated optics has been to provide signal isolation and to suppress parasitic reflections between devices. In this context, there is a very strong interest in the miniaturization of nonreciprocal optical devices and their on-chip integration [18]–[20]. Due to the weakness of magnetooptical effects, conventional devices require a long propagation distance and occupy a large footprint. Thus, it should be very fruitful to explore the enhancement of magnetooptical effects in photonic crystals [21]–[35] for the purpose of creating ultracompact devices with enhanced functionalities.

From a fundamental point of view, the key feature of nonreciprocal photonic crystals is the violation of time-reversal symmetry and reciprocity. As a result, the band structures and the transport properties of photons exhibit characteristics that are completely different from conventional reciprocal systems. Formulating the basic theoretical framework and developing the mathematical techniques and simulation algorithms for such systems are therefore of fundamental importance to understand this new class of photonic crystal structures.

Manuscript received May 24, 2006. This work was supported in part by the National Science Foundation (NSF) and the Defense Advanced Research Projects Agency (DARPA).

The authors are with the Ginzton Laboratory, Stanford University, Stanford, CA 94305 USA.

Color versions of Figs.1–4, and 7 are available at http://ieeexplore.ieee.org.
Digital Object Identifier 10.1109/JLT.2006.886061

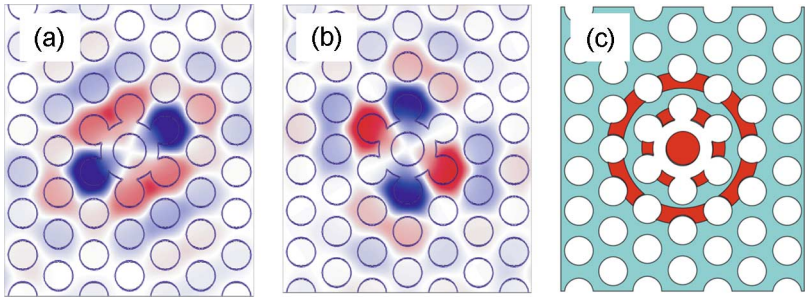

Fig. 1. (a) and (b) Pair of doubly degenerate defect states in a 2-D photonic crystal. The crystal consists of an array of air holes introduced into a high dielectric material. Red and blue represent large positive and negative magnetic fields, respectively. (c) Domain structure that maximizes the magnetooptical coupling between the two defect states in (a) and (b). Cyan and red areas represent regions with magnetization direction along positive and negative directions parallel to the air holes, respectively.

A. Modal Analysis of Magnetooptical Resonators

At optical wavelengths, the property of a magnetooptical material is typically characterized by a gyrotropic dielectric tensor $\overleftrightarrow{\varepsilon}$ [36], i.e.,

$$D = \overleftrightarrow{\varepsilon}\, E = \varepsilon_0 E + j\varepsilon_a \hat{M} \times E \equiv \left(\varepsilon_0 + \overleftrightarrow{\varepsilon'}\right) E \tag{1}$$

where ε_0 is the dielectric constant in the absence of magnetization, ε_a measures the strength of the magnetooptical effects, and $\hat{M}$ is the unit vector indicating the direction of magnetization. When the magnetization is along the z-direction, the dielectric tensor in (1) assumes the following form:

$$\overleftrightarrow{\varepsilon} = \begin{pmatrix} \varepsilon_0 & \pm i\varepsilon_a & 0 \\ \mp i\varepsilon_a & \varepsilon_0 & 0 \\ 0 & 0 & \varepsilon_0 \end{pmatrix} \tag{2}$$

where the magnetization is assumed to be along the z-direction. The off-diagonal elements in (2) have their signs dictated by the direction of magnetization. The strength of magnetooptical effects is measured by the Voigt parameter $Q_M = \varepsilon_a/\varepsilon_0$. For most transparent materials, the Voigt parameter is typically less than 10^{-3} [36].

To theoretically describe modes in a magnetooptical photonic crystal system, we start with the vector wave equations for photonic crystals [4], where the magnetic field H in the steady state at an angular frequency ω is obtained by solving the following eigenvalue equation:

$$\Theta|H\rangle = \nabla\times \overleftrightarrow{\varepsilon}^{-1} \nabla \times |H\rangle = \left(\frac{\omega}{c}\right)^2 |H\rangle. \tag{3}$$

In general, this equation can be solved numerically using existing techniques for photonic crystal band structure calculations [37]. To highlight the essential feature of magnetooptical photonic crystals, however, we take advantage of the fact that the Voigt parameter is very weak to develop a perturbation theory. Starting from (3) and expanding to first order in ε_a, we have

$$\Theta|H\rangle = \nabla \times \frac{1}{\varepsilon_0}\nabla \times |H\rangle - \nabla \times \frac{\overleftrightarrow{\varepsilon'}}{\varepsilon_0^2}\nabla \times |H\rangle = \left(\frac{\omega}{c}\right)^2 |H\rangle. \tag{4}$$

In (4), $\Theta_0 \equiv \nabla \times 1/\varepsilon_0 \nabla\times$ describes a photonic crystal in the absence of magnetooptical effects. The effects of magnetooptics can now be treated in terms of the coupling of eigenmodes of Θ_0 as induced by the perturbation $V \equiv -\nabla \times (\overleftrightarrow{\varepsilon'}/\varepsilon_0^2)\nabla\times$.

For two normalized eigenmodes $|H_{1,2}\rangle$ for Θ_0 at eigenfrequencies $\omega_{1,2}$, the coupling constant between them, as induced by V, can be calculated as

$$\begin{aligned} V_{12} &\equiv \langle H_1|V|H_2\rangle \\ &= -\int H_1^* \cdot \nabla \times \frac{\overleftrightarrow{\varepsilon'}}{\varepsilon_0^2}\nabla \times H_2 \\ &= -\int (\nabla \times H_1^*) \cdot \frac{\overleftrightarrow{\varepsilon'}}{\varepsilon_0^2}(\nabla \times H_2) \\ &= -\omega_1\omega_2 \int E_1^* \cdot \overleftrightarrow{\varepsilon'} \cdot E_2 \\ &= -\omega_1\omega_2 \int E_1^* \cdot j\varepsilon_a \hat{M} \times E_2 \\ &= \omega_1\omega_2 \int j\varepsilon_a \hat{M} \cdot (E_1^* \times E_2)\,. \end{aligned} \tag{5}$$

As a concrete example of some of the physical consequences of magnetooptical coupling, we consider a two-dimensional (2-D) crystal shown in Fig. 1 [9]. The structure consists of a triangular lattice of air holes in bismuth–iron–garnet. The air holes have a radius of $0.35a$, where a is the lattice constant. The corresponding nonmagnetic photonic crystal exhibits a large band gap for TE modes that have electric field polarized in the plane. Filling one of the air holes creates a pair of degenerate dipole modes in the photonic band gap. These two modes can be categorized as an even mode $|e\rangle$ [Fig. 1(a)] and an odd mode $|o\rangle$ [Fig. 1(b)] with respect to a mirror plane of the crystal.

In the presence of magnetooptical materials, the two modes $|e\rangle$ and $|o\rangle$ couple with each other. The system is now described by a 2×2 matrix, i.e.,

$$\Theta = \begin{pmatrix} \omega_e^2 & V_{\rm eo} \\ -V_{\rm eo} & \omega_o^2 \end{pmatrix}. \tag{6}$$

Since the two modes are standing waves that possess real-valued electric fields, the coupling constant $V_{\rm eo}$, as described by (5), is purely imaginary. For this system, which has C_{6v} symmetry, $\omega_e = \omega_o \equiv \omega_0$. With the presence of magnetooptical

materials in the cavity, the eigenmodes of the systems, denoted as $|+\rangle$ and $|-\rangle$, now take the form of a rotating wave, i.e.,

$$|\pm\rangle = |e\rangle \pm i|o\rangle \tag{7}$$

with the frequencies located at

$$\omega_{\pm} = \omega_0 \pm \frac{|V_{\rm eo}|}{2\omega_0}. \tag{8}$$

The above modal analysis reveals some of the most interesting properties about magnetooptical photonic crystals in general.

1) *Time-reversal symmetry breaking*. Since the two counterrotating modes $|\pm\rangle$ are related by a time-reversal operation, the frequency splitting between them clearly indicates the breaking of time-reversal symmetry and reciprocity.
2) *Fundamental suppression of the effects of disorder by time-reversal symmetry breaking*. Even in the case where ω_e deviates from ω_o, for example, due to fabrication-related disorder that breaks the threefold rotational symmetry, as long as the magnetooptical coupling is sufficiently strong, i.e., $|V_{\rm eo}| \gg |\omega_e - \omega_o|\omega_e$, $|e\rangle \pm i|o\rangle$ remain the eigenstates of the system. Thus, in the limit of strong magnetooptical coupling, the rotating waveform of the eigenmodes is independent of the slight structural disorders that would almost always occur in practical devices.
3) *Reconfigurability through domain engineering*. Examining (5), we note that the strength of the magnetooptical coupling is strongly influenced by the magnetic domain structures. The cross product $E_e \times E_o$ changes sign rapidly within the cavity. Thus, a cavity completely covered by a uniform domain structure, in spite of the presence of magnetooptical material, has a very weak magnetooptical coupling strength and essentially behaves as a reciprocal optical resonator. On the other hand, designing the domain structures according to the sign of the modal cross product can maximize the magnetooptical coupling [Fig. 1(c)]. Alternatively, strong coupling can also be achieved with the use of a single domain that covers the center area of the cavity where the modal cross product does not change sign. Rewriting the domain structure alone, as can be accomplished by applying external magnetic field or local heating, can thus reconfigure magnetooptical circuits.

Below, we show that these unique modal properties of magnetooptical photonic crystals lead to remarkable transport properties in ultracompact magnetooptical photonic crystal circuits [10], [11].

B. Ultracompact Magnetooptical Circulator

Exploiting the rotating states inside a magnetooptical photonic crystal cavity, we design a four-port circulator as shown in Fig. 2. The system consists of a bus and a drop waveguide, both evanescently coupled to the resonator. Magnetooptical materials are introduced in the cavity region, in a fashion as discussed in the previous section, to create large magnetooptical coupling between the cavity modes. The resulting cavity modes become two circularly rotating modes in opposite directions at different frequencies. When the magnetooptically induced frequency splitting between the two rotating modes exceeds the cavity linewidth that results from the cavity–waveguide coupling, the device functions as an optical circulator that provides optical signal isolation. Light incident from the waveguide in the lower half of the structure, with a frequency coinciding with the counterclockwise resonance in the cavity, is completely transferred to other waveguide [Fig. 2(a)]. In the time-reversed scenario, the incident light through the upper waveguide remains untransferred since the clockwise rotating resonance in the cavity has a different frequency [Fig. 2(b)]. The device footprint is on the single-micrometer scale, and the device is readily integrated with other planar components.

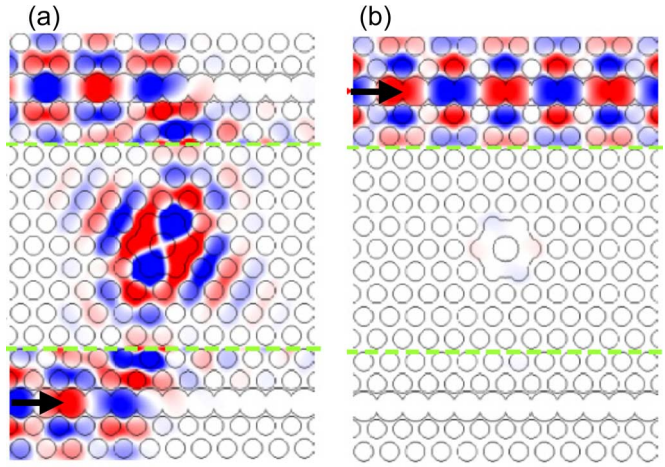

Fig. 2. Operation of a photonic crystal circulator constructed by coupling the magnetooptical cavity as shown in Fig. 1 to two waveguides. Shown here are steady-state field distributions when the incident light is in resonance with the counterclockwise rotating state. Red and blue represent large positive and negative fields, respectively. The arrows indicate the direction of the incident light. The field between two dashed lines are plotted with a different saturation such that fields in both waveguides and cavities can be seen.

C. Suppression of Disorder Effects With Time-Reversal Symmetry Breaking

In Section II-A, we have shown that the form of eigenstates in a magnetooptical resonator is independent of disorder in the strong magnetooptical coupling regime. Here, we explore this modal characteristic in connection with transport properties by considering the disorder tolerance of the circulator structure as presented in the previous section.

To highlight the property of nonreciprocal devices, we have in fact designed the circulator structure such that the device functions as an ideal add–drop filter, when the off-diagonal part of the matrix elements in the dielectric tensor is set to zero. In such a reciprocal add–drop filter, the ideal 100% transfer efficiency relies on creating rotating states from a linear superposition of two degenerate standing-wave modes having the same frequency and linewidth [38]. Preserving the degeneracy condition of the standing-wave modes translates to stringent tolerance requirements. Small fabrication imperfections can easily

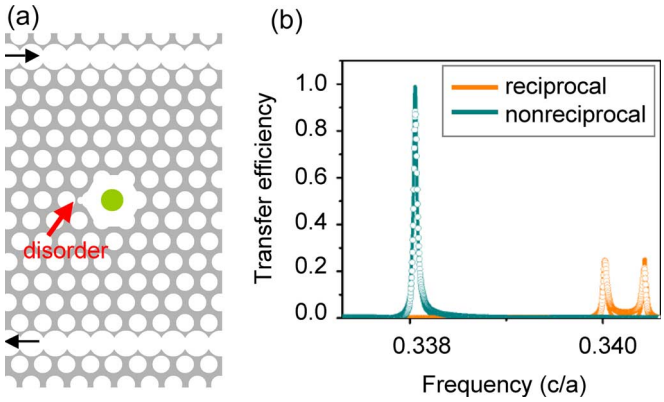

Fig. 3. (a) Photonic crystal circulator structure with two waveguides side-coupled to a cavity at the center. The green region at the center of the cavity consists of magnetooptical material. In the absence of the disorder, in the form of a small bump at the side the cavity, both the circulator structure and its fictitious reciprocal counterpart, created by removing the off-diagonal part of the dielectric tensor, give ideal transfer efficiency between the waveguides at resonance. The black arrows represent the direction of transfer. (b) Comparison of the transfer property of the circulator and its reciprocal counterpart in the presence of the disorder.

split the frequencies of the standing-wave modes, resulting in low transfer efficiency and strong back reflections in the input waveguide. This is demonstrated in Fig. 3, where, as an example of disorder, we introduce a small bump on the side of the cavity. For the reciprocal structure, such a disorder reduces the transfer efficiency between the waveguides from 100% to 25% and causes strong reflection in the incoming waveguide. In the nonreciprocal structure, on the other hand, the peak transmission efficiency remains very close to 100%, in spite of the disorder [11]. We believe that exploring the interplay between time-reversal symmetry breaking and disorder is a particularly exciting area, which can potentially lead to regimes of photon propagation that are completely absent in reciprocal structures.

III. Stopping Light in Dynamic Photonic Crystals

A. Introduction

In this section, we point out the fascinating new possibilities when dynamic behaviors are introduced into the photonic crystal systems. The idea of dynamic photonic crystal is to modulate the property of a crystal while a photon pulse is inside the crystal. In doing so, the spectrum of the pulse can be molded almost arbitrarily with a small refractive index modulation, leading to highly nontrivial information-processing capabilities on chip. As examples of such capabilities, we show that the bandwidth of a light pulse can be compressed to zero, resulting in all-optical stopping and storage of light [12]–[17]. The spectrum of a light pulse can also be inverted to give a time-reversal operation [13], [14].

A fundamental difficulty in integrated optics has been that different optical functionalities tend to require different material systems. For example, the traditional way to accomplish time-reversal through phase conjugation requires nonlinear optical materials such as $LiNbO_3$ [39]. In addition, light stopping has been demonstrated only in atomic gases under extreme conditions [40], [41]. On the other hand, small refractive index modulations required to create dynamic photonic crystal can be readily incorporated in standard optoelectronic systems. Thus, the use of dynamic photonic structures, as we envision here, may provide a unifying platform for diverse optical information-processing tasks in the future.

B. Tuning the Spectrum of Light

Here, we provide a simple example to show how the spectrum of electromagnetic wave can be modified by a dynamic photonic structure. Consider a linearly polarized electromagnetic wave in one dimension. The wave equation for the electric field is

$$\frac{\partial^2 E}{\partial x^2} - (\varepsilon_0 + \varepsilon(t))\,\mu_0 \frac{\partial^2 E}{\partial t^2} = 0. \tag{9}$$

Here, $\varepsilon(t)$ represents the modulation, and ε_0 is the background dielectric constant. We assume that both ε_0 and $\varepsilon(t)$ are independent of position. Hence, different wavevector components do not mix in the modulation process. For a specific wavevector component at k_0, with electric field described by $E(t) = f(t)e^{i(\omega_0 t - k_0 x)}$, where $\omega_0 = k_0/\sqrt{\mu_0\varepsilon_0}$, we have

$$-k_0^2 f - [\varepsilon_0 + \varepsilon(t)]\,\mu_0 \left[\frac{\partial^2 f}{\partial t^2} + 2i\omega_0 \frac{\partial f}{\partial t} - \omega_0^2 f\right] = 0. \tag{10}$$

By using a slowly varying envelope approximation, i.e., ignoring the $\partial^2 f/\partial t^2$ term, and by further assuming that the index modulations are weak, i.e., $\varepsilon(t) \ll \varepsilon_0$, (10) can be simplified as

$$i\frac{\partial f}{\partial t} = \frac{\varepsilon(t)\omega_0}{2\,[\varepsilon(t) + \varepsilon_0]} f \approx \frac{\varepsilon(t)\omega_0}{2\varepsilon_0} f \tag{11}$$

which has an exact analytic solution, i.e.,

$$f(t) \ll f(t_0) \exp\left[-i\omega_0 \int_{t_0}^{t} \frac{\varepsilon(t')}{2\varepsilon_0} dt'\right] \tag{12}$$

where t_0 is the starting time of the modulation. Thus, the "instantaneous frequency" of the electric field for this wavevector component is

$$\omega(t) = \omega_0 \left(1 - \frac{\varepsilon(t)}{2\varepsilon_0}\right). \tag{13}$$

We note that frequency change is proportional to the magnitude of the refractive index shift alone. Thus, the process defined here differs in a fundamental way from traditional nonlinear optical processes. For example, in a conventional sum frequency conversion process, to convert the frequency of light from ω_1 to ω_2, modulations at a frequency $\omega_2 - \omega_1$ need to be provided. In contrast, in the process described here, regardless of how slow the modulation is, as long as light is in the system, the frequency shift can always be accomplished. Below, we will demonstrate some very spectacular consequences of

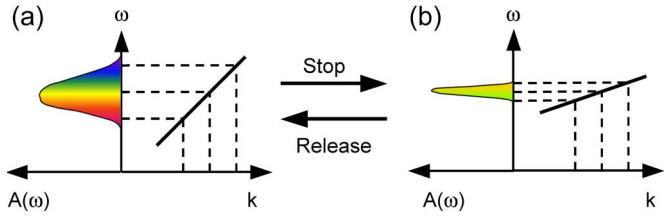

Fig. 4. General conditions for stopping a light pulse. (a) Large-bandwidth state that is used to accommodate an incident light pulse. (b) Narrow-bandwidth state that is used to hold the light pulse. An adiabatic transition between these two states stops a light pulse inside the system.

such frequency shift in the dynamic photonic crystal, in its application for stopping a light pulse all optically.

The existence of the frequency shift in dynamic photonic crystal structures was also pointed out in the studies of photonic crystals in the presence of shock waves [42]. The shock waves, effectively speaking, induce a large refractive index shift. In practical optoelectronic or nonlinear optical devices, on the other hand, the accomplishable refractive index shift is generally quite small. Thus, in most practical situations, the effect of dynamics is prominent only in structures in which the spectral feature is sensitive to small refractive index modulations. This motivates our design on Fano interference schemes, described below, which are employed to enhance the sensitivity of photonic structures to small index modulations.

C. General Conditions for Stopping Light

By stopping light, we aim to reduce the group velocity of a light pulse to zero while completely preserving all the coherent information encoded in the pulse. Such ability holds the key to the ultimate control of light and has profound implications for optical communications and quantum information processing.

There has been extensive work attempting to control the speed of light using optical resonances in static photonic crystal structures. Group velocities as low as $10^{-2}c$ for pulse propagation with negligible distortion have been experimentally observed in waveguide band edges or with coupled resonator optical waveguides (CROWs) [43]–[47]. Nevertheless, such structures are fundamentally limited by the delay–bandwidth product constraint. The group delay from an optical resonance is inversely proportional to the bandwidth within which the delay occurs [48], [49]. Therefore, for a given optical pulse with a certain temporal duration and corresponding frequency bandwidth, the minimum group velocity achievable is limited. In a CROW waveguide structure, for example, the minimum group velocity that can be accomplished for pulses at 10-Gb/s rate with a wavelength of 1.55 μm is no smaller than $10^{-2}c$. For this reason, static photonic structures could not be used to stop light.

To stop light, it is therefore necessary to use a dynamic system. The general condition for stopping light [12] is illustrated in Fig. 4. Imagine a dynamic photonic crystal system with an initial band structure possessing a sufficiently wide bandwidth. Such a state is used to accommodate an incident pulse for which each frequency component occupies a unique wavevector component. After the pulse has entered the system, one can then stop the pulse by flattening the dispersion relation of the crystal adiabatically while preserving the translational invariance. In doing so, the spectrum of the pulse is compressed, and its group velocity is reduced. In the meantime, since the translational symmetry is still preserved, the wavevector components of the pulse remain unchanged, and thus, one actually preserves the dimensionality of the phase space. This is crucial in preserving all the coherent information encoded in the original pulse during the dynamic process.

D. Tunable Fano Resonance

To create a dynamic photonic crystal, one needs to adjust its properties as a function of time. This can be accomplished by modulating the refractive index either with electrooptic or nonlinear optic means. However, the amount of refractive index tuning that can be accomplished with standard optoelectronics technology is generally quite small, with a fractional change typically on the order of $\delta n/n = 10^{-4}$. Therefore, we employ Fano interference schemes in which a small refractive index modulation leads to a very large change of the bandwidth of the system. The essence of Fano interference scheme is the presence of multipath interference, where at least one of the paths includes a resonant tunneling process [50]. Such interference can be used to greatly enhance the sensitivity of resonant devices to small refractive index modulation [15], [51], [52].

Here, we consider a waveguide side-coupled to two cavities [53]. The cavities have resonant frequencies $\omega_{A,B} \equiv \omega_0 \pm (\delta\omega/2)$, respectively. (This system represents an all-optical analogue of atomic systems exhibiting electromagnetically induced transparency (EIT) [54]. Each optical resonance here is analogous to the polarization between the energy levels in the EIT system [55].) For simplicity, we assume that the cavities couple to the waveguide with equal rate of γ, and we ignore the direct coupling between the side cavities. Consider a mode in the waveguide passing through the cavities. The transmission and reflection coefficients ($t_{A,B}$ and $r_{A,B}$, respectively) with a single-sided cavity can then be derived using the Green's function method [56] as

$$t_{A,B} = \frac{j(\omega - \omega_{A,B})}{j(\omega - \omega_{A,B}) + \gamma} \tag{14}$$

$$r_{A,B} = \frac{\gamma}{j(\omega - \omega_{A,B}) + \gamma}. \tag{15}$$

When two cavities are cascaded together, the transmission spectrum can be derived as [57]

$$T = \left(\frac{|t_A t_B|}{1 - |r_A r_B|}\right)^2 \frac{1}{1 + 4\left(\frac{\sqrt{|r_A r_B|}}{1-|r_A r_B|}\right)^2 \sin^2\theta}. \tag{16}$$

θ is one-half of the round-trip phase accumulated in the waveguides: $\theta = (1/2)\mathrm{Arg}[r_A r_B e^{-2j\beta(\omega)L_1}]$, where $\beta(\omega)$ is the waveguide dispersion relationship, and L_1 is the spacing between the cavities.

The transmission spectra of one- and two-cavity structures, calculated using (14)–(16), are plotted in Fig. 5. In the case

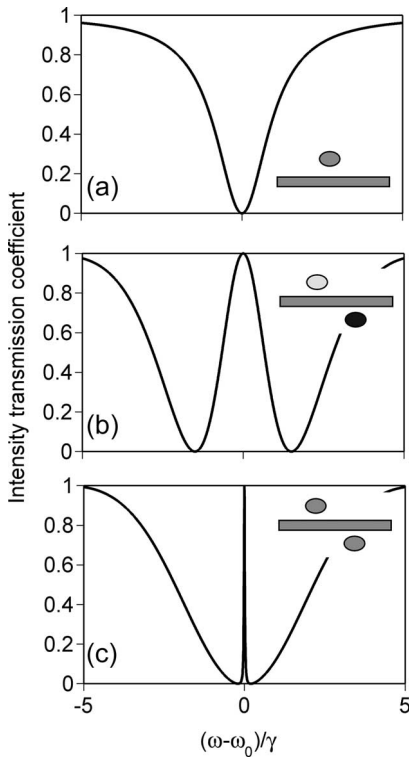

Fig. 5. (a) Transmissions spectrum through a waveguide side-coupled to a single-mode cavity. (b) and (c) Transmission spectra through a waveguide side-coupled to two cavities. The spectra are calculated using (14)–(16). The parameters for the cavities are $\omega_0 = 2\pi c/L_1$ and $\gamma = 0.05\omega_0$. In addition, the waveguide satisfies a dispersion relation $\beta(\omega) = \omega/c$, where c is the speed of light in the waveguide, and L_1 is the distance between the cavities. In (b), $\omega_{A,B} = \omega_0 \pm 1.5\gamma$. In (c), $\omega_{A,B} = \omega_0 \pm 0.2\gamma$.

of one-cavity structure, the transmission features a dip in the vicinity of the resonant frequency, with the width of the dip controlled by the strength of waveguide–cavity coupling [Fig. 5(a)]. With two cavities, when the condition

$$2\beta(\omega_0)L = 2n\pi \tag{17}$$

is satisfied, the transmission spectrum features a peak centered at ω_0. The width of the peak is highly sensitive to the frequency spacing between the resonances $\delta\omega$. When the cavities are lossless, the center peak can be tuned from a wide peak when $\delta\omega$ is large [Fig. 5(b)] to a peak that is arbitrarily narrow with $\delta\omega \to 0$ [Fig. 5(c)]. The two-cavity structure, appropriately designed, therefore behaves as a tunable bandwidth filter (as well as a tunable delay element), in which the bandwidth can be, in principle, adjusted by any order of magnitude with very small refractive index modulation.

E. From Tunable Bandwidth Filter to Light-Stopping System

By cascading the tunable bandwidth filter structure as described in the previous section, one can construct a structure that is capable of stopping light [Fig. 6(a)]. In such a light-stopping structure, the photonic band diagram becomes highly sensitive to small refractive index modulation.

The photonic bands for the structure in Fig. 6(a) can be calculated using a transmission matrix method. The transmission

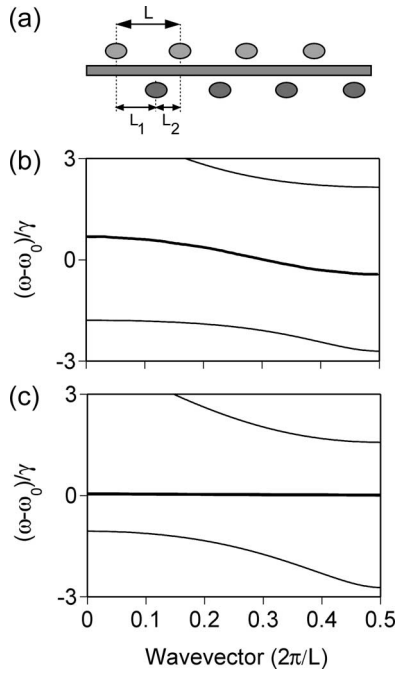

Fig. 6. (a) Schematic of a coupled-cavity structure used to stop light. (b) and (c) Band structures for the system shown in (a), as the frequency separation between the cavities are varied, using the same waveguide and cavity parameters as in Fig. 5(b) and (c), with the additional parameter $L_2 = 0.7L_1$. The thicker lines highlight the middle band that will be used to stop a light pulse.

matrix for a waveguide side-coupled to a single resonator with resonance frequency ω_i can be calculated as [56]

$$T_{c_i} = \begin{pmatrix} 1 + j\gamma/(\omega - \omega_i) & j\gamma/(\omega - \omega_i) \\ -j\gamma/(\omega - \omega_i) & 1 - j\gamma/(\omega - \omega_i) \end{pmatrix}. \tag{18}$$

The transmission matrix through an entire unit cell in Fig. 6 can then be determined as

$$T = T_{c_1} T_{l_1} T_{c_2} T_{l_2} \tag{19}$$

where $T_{l_i} = \begin{pmatrix} e^{-j\beta L_i} & 0 \\ 0 & e^{j\beta L_i} \end{pmatrix}$ is the transmission matrix for a waveguide section of length L_i. Here, β is the wavevector of the waveguide at a given frequency ω.

Since $\det(T) = 1$, the eigenvalues of T can be represented as e^{ikl} and e^{-ikl}, where $L = L_1 + L_2$ is the length of the unit cell, and k (when it is real) corresponds to the Bloch wavevector of the entire system. Therefore, we obtain the band diagram of the system as [14]

$$\begin{aligned} \frac{1}{2}Tr(T) &= \cos(kL) = f(\omega) \\ &\equiv \cos(\beta L) + \frac{C_+}{(\omega - \omega_A)} + \frac{C_-}{(\omega - \omega_B)} \end{aligned} \tag{20}$$

where $C_\pm = \gamma \sin(\beta L) \pm \gamma^2[2\sin(\beta L_1)\sin(\beta L_2)/(\omega_A - \omega_B)]$. In the frequency range where $|f(\omega)| < 1$, the system supports propagating modes, whereas $|f(\omega)| > 1$ corresponds to the frequency ranges of the photonic band gaps.

The band diagrams thus calculated are shown in Fig. 6, in which the waveguide and cavity parameters are the same as those used to generate the transmission spectrum in Fig. 5. In the vicinity of the resonances, the system supports three photonic bands, with two gaps occurring around ω_A and ω_B. The width of the middle band depends strongly on the resonant frequencies ω_A and ω_B. By modulating the frequency spacing between the cavities, one goes from a system with a large bandwidth [Fig. 6(b)] to a system with a very narrow bandwidth [Fig. 6(c)]. In fact, it can be analytically proved that the system can support a band that is completely flat in the entire first Brillouin zone [14], allowing a light pulse to be frozen inside the structure with the group velocity reduced to zero. Moreover, the gaps surrounding the middle band have sizes on the order of the cavity–waveguide coupling rate γ and are approximately independent of the slope of the middle band. Thus, by increasing the waveguide–cavity coupling rate, this gap can be made large, which is important for preserving the coherent information during the dynamic bandwidth compression process [12].

F. Numerical Demonstration in a Photonic Crystal

The system presented above can be implemented in a photonic crystal of a square lattice of dielectric rods $(n = 3.5)$ with a radius of $0.2a$ (a is the lattice constant) embedded in air $(n = 1)$ [14] (Fig. 7). The photonic crystal possesses a band gap for TM modes with electric field parallel to the rod axis. Removing one row of rods along the pulse propagation direction generates a single-mode waveguide. Decreasing the radius of a rod to $0.1a$ and the dielectric constant to $n = 2.24$ provides a single-mode cavity with resonance frequency at $\omega_c = 0.357 \cdot (2\pi c/a)$. The nearest neighbor cavities are separated by a distance of $l_1 = 2a$ along the propagation direction, and the unit cell periodicity is $l = 8a$. The waveguide–cavity coupling occurs through barrier of one rod, with a coupling rate of $\gamma = \omega_c/235.8$. The resonant frequencies of the cavities are tuned by refractive index modulation of the cavity rods.

We simulate the entire process of stopping light for $N = 100$ pairs of cavities with finite-difference time-domain (FDTD) method, which solves Maxwell's equations without approximation. The dynamic process for stopping light is shown in Fig. 7. We generate a Gaussian pulse in the waveguide. (The process is independent of the pulse shape.) The excitation reaches its peak at $t = 0.8t_{\text{pass}}$, where t_{pass} is the traversal time of the pulse through the static structure. During the pulse generation, the cavities have a large frequency separation. The field is concentrated in both the waveguide and the cavities [see Fig. 7(b), $t = 1.0t_{\text{pass}}$], and the pulse propagates at a relatively high speed of $v_g = 0.082c$. After the pulse is generated, we gradually reduce the frequency separation Δ to zero. During this process, the speed of light is drastically reduced to zero. As the bandwidth of the pulse is reduced, the field concentrates in the cavities [see Fig. 7(b), $t = 5.2t_{\text{pass}}$]. When zero group velocity is reached, the photon pulse can be kept in the system as a stationary waveform for any time duration. In this simulation, we store the pulse for a time delay of $5.0t_{\text{pass}}$ and then release the pulse by repeating the same index modulation in reverse [see Fig. 7(b), $t = 6.3t_{\text{pass}}$]. The pulse intensity as a function of time at the right end of the waveguide is plotted in Fig. 3(a) and shows the same temporal shape as both the pulse that propagates through the unmodulated system and the initial pulse recorded at the left end of the waveguide. Thus, the pulse is perfectly recovered without distortion after the intended delay.

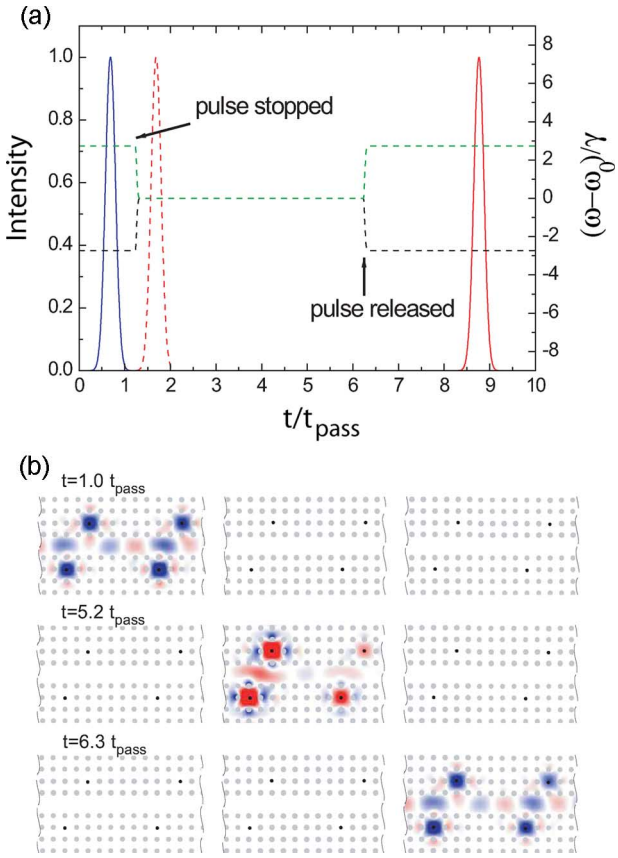

Fig. 7. Light-stopping process in a photonic crystal simulated using FDTD methods. The crystal consists of a waveguide side-coupled to 100 cavity pairs. Fragments of the photonic crystal are shown in (b). The three fragments correspond to unit cells 12-13, 55-56, and 97-98. The dots indicate the positions of the dielectric rods. The black dots represent the cavities. (a) Dashed green and black lines represent the variation of ω_A and ω_B as a function of time, respectively. The blue solid line is the intensity of the incident pulse as recorded at the beginning of the waveguide. The red dashed and solid lines represent the intensity at the end of the waveguide in the absence and presence of modulation, respectively. t_{pass} is the passage time of the pulse in the absence of modulation. (b) Snapshots of the electric field distributions in the photonic crystal at the indicated times. Red and blue represent large positive and negative electric fields, respectively. The same color scale is used for all the panels.

G. Future Prospects of Dynamic Photonic Crystal System

In the all-optical light-stopping scheme presented above, for a small refractive index shift of $\delta n/n = 10^{-4}$ achievable in practical optoelectronic devices, and assuming a carrier frequency of approximately 200 THz, as used in optical communications, the achievable bandwidths are on the order of 20 GHz, which is comparable to the bandwidth of a single-wavelength channel in high-speed optical systems. The storage times are limited only by the cavity lifetimes, which may eventually approach millisecond timescales as limited by residual loss in transparent materials. The loss in optical resonator systems

might be further counteracted with the use of gain media in the cavities or with external amplification. With such performance, the capabilities for on-chip stopping light should have important implications for optical communication systems. As an important step toward its eventual experimental demonstration, the required EIT-like two-cavity interference effects have recently been observed in a microring cavity system on a silicon chip [57]. The general concept of introducing dynamics into photonic crystal systems could also be very promising for creating new optical signal processing functionalities far beyond the capabilities of static systems.

IV. Concluding Remarks

In this paper, we provide a glimpse of recent developments in the theory of photonic crystals, drawing examples from our own recent work on magnetooptical as well as dynamic crystal structures. These developments highlight two general trends in the theoretical work in this field. On one hand, using computational electromagnetic techniques such as the FDTD methods [58] in combination with modern large-scale computing architectures, almost any complex optical processes in photonic crystal can now be simulated through exact numerical solutions of Maxwell's equations. On the other hand, with the band structures and modal properties of passive dielectric photonic structures largely mapped out, one can now create analytic models with only a few dynamic variables based on these modal properties to describe the essential physics of optical processes in photonic crystals. These developments in both theory and simulations, in the context of very rapid progress in experimental fabrications of photonic crystals, are leading to ways of controlling light that are truly unprecedented.

References

[1] E. Yablonovitch, "Inhibited spontaneous emission in solid state physics and electronics," *Phys. Rev. Lett.*, vol. 58, no. 20, pp. 2059–2062, May 1987.

[2] S. John, "Strong localization of photons in certain disordered dielectric superlattices," *Phys. Rev. Lett.*, vol. 58, no. 23, pp. 2486–2489, Jun. 1987.

[3] A. Mekis, J. C. Chen, I. Kurland, S. Fan, P. R. Villeneuve, and J. D. Joannopoulos, "High transmission through sharp bends in photonic crystal waveguides," *Phys. Rev. Lett.*, vol. 77, no. 18, pp. 3787–3790, Oct. 1996.

[4] J. D. Joannopoulos, R. D. Meade, and J. N. Winn, *Photonic Crystals: Molding the Flow of Light*. Princeton, NJ: Princeton Univ. Press, 1995.

[5] J. D. Joannopoulos, P. R. Villeneuve, and S. Fan, "Photonic crystals: Putting a new twist on light," *Nature*, vol. 386, no. 6621, pp. 143–147, 1997.

[6] *Photonic Crystals and Light Localization in the 21st Century*, C. Soukoulis, Ed. Dordrecht, The Netherlands: Kluwer, 2001. NATO ASI Series.

[7] S. G. Johnson and J. D. Joannopoulos, *Photonic Crystals: The Road From Theory to Practice*. Boston, MA: Kluwer, 2002.

[8] K. Inoue and K. Ohtaka, *Photonic Crystals*. Berlin, Germany: Springer-Verlag, 2004.

[9] Z. Wang and S. Fan, "Magneto-optical defects in two-dimensional photonic crystals," *Appl. Phys. B, Photophys. Laser Chem.*, vol. 81, no. 2/3, pp. 369–375, 2005.

[10] ——, "Optical circulators in two-dimensional magneto-optical photonic crystals," *Opt. Lett.*, vol. 30, no. 15, pp. 1989–1991, Aug. 2005.

[11] ——, "Add–drop filter in two-dimensional magneto-optical photonic crystals and suppression of disorder effects by time-reversal breaking," *Photon. Nanostruct.: Fundam. Appl.* (in press).

[12] M. F. Yanik and S. Fan, "Stopping light all-optically," *Phys. Rev. Lett.*, vol. 92, no. 8, p. 083901, Feb. 2004.

[13] ——, "Time-reversal of light with linear optics and modulators," *Phys. Rev. Lett.*, vol. 93, no. 17, p. 173 903, Oct. 2004.

[14] M. F. Yanik, W. Suh, Z. Wang, and S. Fan, "Stopping light in a waveguide with an all-optical analogue of electromagnetically induced transparency," *Phys. Rev. Lett.*, vol. 93, no. 23, p. 233 903, Dec. 2004.

[15] M. F. Yanik and S. Fan, "Stopping and storing light coherently," *Phys. Rev. A, Gen. Phys.*, vol. 71, no. 1, p. 013803, Jan. 2005.

[16] ——, "Dynamic photonic structures: Stopping, storage, and time-reversal of light," *Stud. Appl. Math.*, vol. 115, no. 2, pp. 233–254, 2005.

[17] S. Sandhu, M. L. Povinelli, M. F. Yanik, and S. Fan, "Dynamically-tuned coupled resonator delay lines can be nearly dispersion free," *Opt. Lett.*, vol. 31, no. 13, pp. 1985–1987, Jul. 2006.

[18] M. Levy, "The on-chip integration of magneto-optic waveguide isolators," *IEEE J. Sel. Topics Quantum Electron.*, vol. 8, no. 6, pp. 1300–1306, Nov./Dec. 2002.

[19] R. L. Espinola, T. Izuhara, M. Tsai, R. M. Osgood, and H. Dotsch, "Magneto-optical nonreciprocal phase shift in garnet/silicon-on-insulators waveguides," *Opt. Lett.*, vol. 29, no. 9, pp. 941–943, May 2004.

[20] H. Yokoi, Y. Shoji, E. Shin, and T. Mizumoto, "Interferometric optical isolator employing a non-reciprocal phase shift operated in a unidirectional magnetic field," *Appl. Opt.*, vol. 43, no. 24, pp. 4745–4752, Aug. 2004.

[21] M. Inoue, K. Arai, T. Fujii, and M. Abe, "One-dimensional magnetophotonic crystals," *J. Appl. Phys.*, vol. 85, no. 8, pp. 5768–5770, Apr. 1999.

[22] E. Takeda, N. Todoroki, Y. Kitamoto, M. Abe, M. Inoue, T. Fujii, and K. Arai, "Faraday effect enhancement in co-ferrite layer incorporated into one-dimensional photonic crystal working as a Fabry–Pérot resonator," *J. Appl. Phys.*, vol. 87, no. 9, pp. 6782–6784, May 2000.

[23] M. J. Steel, M. Levy, and R. M. Osgood, "High transmission enhanced Faraday rotation in one-dimensional photonic crystal with defects," *IEEE Photon. Technol. Lett.*, vol. 12, no. 9, pp. 1171–1173, Sep. 2000.

[24] A. Figotin and I. Vitebsky, "Nonreciprocal magnetic photonic crystals," *Phys. Rev. E, Stat. Phys. Plasmas Fluids Relat. Interdiscip. Top.*, vol. 63, no. 6, p. 066609, Jun. 2001.

[25] A. Figotin and I. Vitebskiy, "Electromagnetic unidirectionality in magnetic photonic crystals," *Phys. Rev. B, Condens. Matter*, vol. 67, no. 16, p. 165 210, Apr. 2003.

[26] A. A. Jalali and A. T. Friberg, "Faraday rotation in a two-dimensional photonic crystal with a magnetooptic defect," *Opt. Lett.*, vol. 30, no. 10, pp. 1213–1215, May 2005.

[27] R. Li and M. Levy, "Bragg grating magnetic photonic crystal waveguides," *Appl. Phys. Lett.*, vol. 86, no. 25, p. 251 102, Jun. 2005.

[28] Y. Ikezawa, K. Nishimura, H. Uchida, and M. Inoue, "Preparation of two-dimensional magneto-photonic crystals of bismuth substitute yttrium iron garnet materials," *J. Magn. Magn. Mater.*, vol. 272–276, pp. 1690–1691, May 2004.

[29] K. Nishimura, A. V. Baryshev, T. Kodama, H. Uchida, and M. Inoue, "Synthesis of ferrite on SiO_2 sphere for three-dimensional magneto-photonic crystals," *J. Appl. Phys.*, vol. 95, no. 11, pp. 6633–6635, Jan. 2004.

[30] C. Koerdt, G. L. J. A. Rikken, and E. P. Petrov, "Faraday effect of photonic crystals," *Appl. Phys. Lett.*, vol. 82, no. 10, pp. 1538–1540, Mar. 2003.

[31] A. K. Zvezdin and V. I. Belotelov, "Magneto-optical properties of two dimensional photonic crystals," *Eur. Phys. J. B*, vol. 37, no. 4, pp. 479–487, 2004.

[32] N. Kono and Y. Tsuji, "A novel finite-element method for nonreciprocal magneto-photonic crystal waveguides," *J. Lightw. Technol.*, vol. 22, no. 7, pp. 1741–1747, Jul. 2004.

[33] N. Kono and M. Koshiba, "General finite-element modeling of 2-D magneto-photonic crystal waveguides," *IEEE Photon. Technol. Lett.*, vol. 17, no. 7, pp. 1432–1434, Jul. 2005.

[34] S. K. Mondal and B. J. H. Stadler, "Novel designs for integrating YIG/air photonic crystal slab polarizers with waveguide Faraday rotators," *IEEE Photon. Technol. Lett.*, vol. 17, no. 1, pp. 127–129, Jan. 2005.

[35] N. Kono and M. Koshiba, "Three-dimensional finite-element analysis of non-reciprocal phase shifts in magneto-photonic crystal waveguides," *Opt. Express*, vol. 13, no. 23, p. 9155, Nov. 2005.

[36] A. K. Zvezdin and V. A. Kotov, *Modern Magnetooptics and Magnetooptical Materials*. Bristol, U.K.: Inst. Phys., 1997.

[37] S. G. Johnson and J. D. Joannopoulos, "Block-iterative frequency-domain methods for Maxwell's equations in a planewave basis," *Opt. Express*, vol. 8, no. 3, pp. 173–190, Jan. 2001.

[38] S. Fan, P. R. Villeneuve, J. D. Joannopoulos, and H. A. Haus, "Channel drop tunneling through localized states," *Phys. Rev. Lett.*, vol. 80, no. 5, pp. 960–963, Feb. 1998.

[39] D. Psaltis, "Coherent optical information systems," *Science*, vol. 298, no. 5597, pp. 1359–1363, Nov. 2002.

[40] C. Liu, Z. Dutton, C. H. Behroozi, and L. V. Hau, "Observation of coherent optical information storage in an atomic medium using halted light pulses," *Nature*, vol. 409, no. 6819, pp. 490–493, Jan. 2001.
[41] D. F. Phillips, A. Fleischhauer, A. Mair, R. L. Walsworth, and M. D. Lukin, "Storage of light in atomic vapors," *Phys. Rev. Lett.*, vol. 86, no. 5, pp. 783–786, Jan. 2001.
[42] E. J. Reed, M. Soljacic, and J. D. Joannopoulos, "Color of shock waves in photonic crystals," *Phys. Rev. Lett.*, vol. 90, no. 20, p. 203 904, May 2003.
[43] M. Notomi, K. Yamada, A. Shinya, J. Takahashi, C. Takahashi, and I. Yokoyama, "Extremely large group-velocity dispersion of line-defect waveguides in photonic crystal slabs," *Phys. Rev. Lett.*, vol. 87, no. 25, p. 253 902, Dec. 2001.
[44] N. Stefanou and A. Modinos, "Impurity bands in photonic insulators," *Phys. Rev. B, Condens. Matter*, vol. 57, no. 19, pp. 12127–12133, 1998.
[45] A. Yariv, Y. Xu, R. K. Lee, and A. Scherer, "Coupled-resonator optical waveguide: A proposal and analysis," *Opt. Lett.*, vol. 24, no. 11, pp. 711–713, Jun. 1999.
[46] M. Bayindir, B. Temelkuran, and E. Ozbay, "Tight-binding description of the coupled defect modes in three-dimensional photonic crystals," *Phys. Rev. Lett.*, vol. 84, no. 10, pp. 2140–2143, Mar. 2000.
[47] Y. A. Vlasov, M. O'Boyle, H. F. Harmann, and S. J. McNab, "Active control of slow light on a chip with photonic crystal waveguides," *Nature*, vol. 438, no. 7064, pp. 65–69, Nov. 2005.
[48] G. Lenz, B. J. Eggleton, C. K. Madsen, and R. E. Slusher, "Optical delay lines based on optical filters," *IEEE J. Quantum Electron.*, vol. 37, no. 4, pp. 525–532, Apr. 2001.
[49] Z. Wang and S. Fan, "Compact all-pass filters in photonic crystals as the building block for high capacity optical delay lines," *Phys. Rev. E, Stat. Phys. Plasmas Fluids Relat. Interdiscip. Top.*, vol. 68, no. 6, p. 066616, Dec. 2003.
[50] U. Fano, "Effects of configuration interaction on intensities and phase shifts," *Phys. Rev.*, vol. 124, no. 6, pp. 1866–1878, Dec. 1961.
[51] S. Fan, "Sharp asymmetric lineshapes in side-coupled waveguide–cavity systems," *Appl. Phys. Lett.*, vol. 80, no. 6, pp. 908–910, Feb. 2002.
[52] S. Fan, W. Suh, and J. D. Joannopoulos, "Temporal coupled mode theory for Fano resonances in optical resonators," *J. Opt. Soc. Amer. A, Opt. Image Sci.*, vol. 20, no. 3, pp. 569–572, Mar. 2003.
[53] W. Suh, Z. Wang, and S. Fan, "Temporal coupled-mode theory and the presence of non-orthogonal modes in lossless multi-mode cavities," *IEEE J. Quantum Electron.*, vol. 40, no. 10, pp. 1511–1518, Oct. 2004.
[54] S. E. Harris, "Electromagnetically induced transparency," *Phys. Today*, vol. 50, no. 7, pp. 36–42, 1997.
[55] L. Maleki, A. B. Matsko, A. A. Savchenkov, and V. S. Ilchenko, "Tunable delay line with interacting whispering-gallery-mode resonators," *Opt. Lett.*, vol. 29, no. 6, pp. 626–628, Mar. 2004.
[56] S. Fan, P. R. Villeneuve, J. D. Joannopoulos, C. Manalatou, M. J. Khan, and H. A. Haus, "Theoretical investigation of channel drop tunneling processes," *Phys. Rev. B, Condens. Matter*, vol. 59, no. 24, pp. 15 882–15 892, Jun. 1999.
[57] Q. Xu, S. Sandhu, M. L. Povinelli, J. Shakya, S. Fan, and M. Lipson, "Experimental realization of an on-chip all-optical analogue to electromagnetically induced transparency," *Phys. Rev. Lett.*, vol. 96, no. 12, p. 123 901, Mar. 2006.
[58] A. Taflove and S. C. Hagness, *Computational Electrodynamics: The Finite-Difference Time-Domain Method*. Norwood, MA: Artech House, 2005.

Shanhui Fan (SM'06) received the Ph.D. degree in theoretical condensed matter physics from the Massachusetts Institute of Technology (MIT), Cambridge, in 1997.

He is an Assistant Professor of electrical engineering with Stanford University, Stanford, CA. He was a Research Scientist with the Research Laboratory of Electronics, MIT, prior to his appointment at Stanford. He has published more than 120 refereed journal articles and has given more than 80 invited talks. He is the holder of 24 U.S. patents. His research interests are in computational and theoretical studies of solid-state and photonic structures and devices, especially photonic crystals, microcavities, and nanophotonic circuits and elements.

Prof. Fan is a member of the Optical Society of America, the American Physical Society, and the International Society for Optical Engineering (SPIE). He was a recipient of a National Science Foundation Career Award and a David and Lucile Packard Fellowship in Science and Engineering.

Mehmet Fatih Yanik received the B.S. and M.S. degrees in electrical engineering and physics from the Massachusetts Institute of Technology (MIT), Cambridge, in 1999 and 2000, respectively, and the Ph.D. degree in applied physics from S. Fan's Group, Stanford University, Stanford, CA, in 2006. He completed his short postdoctoral research in bioengineering with S. Quake's Group, Stanford University.

He briefly worked on quantum computing at Xerox Parc and on molecular electronics at HP Laboratories with S. Williams. He is currently an Assistant Professor of electrical engineering with MIT and a Faculty Member of the MIT Computational and Systems Biology Program. His research interests include femtosecond laser nanosurgery, micro- and nanomanipulation, nerve regeneration and degeneration, subdiffraction limit imaging, microfluidics, and nanophotonic devices.

Dr. Yanik was a recipient of the MIT-Chorafas Best Thesis Award for his thesis work with R. Ram at MIT on ultrafast spin spectroscopy. During his Ph.D. study with S. Fan, he received the Stanford Graduate Fellowship Award and the Intel Fellowship Award and showed all-optical coherent photon storage, which was selected among the top ten research advances of the year by *Technology Research News Magazine* in 2004. His studies on nanophotonic devices were awarded the first place in the 2004 Innovator's Challenge Competition in Silicon Valley. He has been selected the "The Outstanding Young Person" by the Junior Chamber International's Branch in 2004.

Zheng Wang (S'03) received the B.S. degree in physics from the University of Science and Technology of China, Hefei, China, in 2000 and the Ph.D. degree in applied physics from Stanford University, Stanford, CA, in 2006.

Since 2006, he has been a Postdoctoral Researcher with the Research Laboratory of Electronics, Massachusetts Institute of Technology, Cambridge. His current research interests focus on microstructure fibers and nonreciprocal photonic circuits.

Sunil Sandhu was born in Singapore. He received the B.Sc. degree in electrical engineering from Christian Brothers University, Memphis, TN, in 1998 and the M.Sc. degree from Stanford University, Stanford, CA, in 2003.

From 1998 to 1999, he worked on telecommunication networks as a Research Assistant with ESIGELEC, Rouen, France. From 2000 to 2002, he worked on optical amplifiers with Onetta, Sunnyvalle, CA. He has been working with Prof. S. Fan as a Research Assistant with the Department of Electrical Engineering, Stanford University, since 2004. His research interests include the dynamic manipulation of light in photonic crystals.

Michelle L. Povinelli received the B.A. degree (Hons.) from the University of Chicago, Chicago, IL, in 1997, the M.Phil. degree from the University of Cambridge, Cambridge, U.K., in 1998, and the Ph.D. degree from the Massachusetts Institute of Technology (MIT), Cambridge, in 2004, all in physics.

She is currently a Postdoctoral Researcher with the Department of Electrical Engineering, Stanford University, Stanford, CA, studying slow light in photonic crystals. She has published more than 15 technical papers. She is the holder of two U.S. patents.

Dr. Povinelli was selected for the Churchill Fellowship, which is an award given to ten American students per year to study at the University of Cambridge, in 1997. She was awarded several graduate fellowships for her doctoral work, including the Lucent Technologies Graduate Research Program for Women (GRPW) Fellowship, the National Science Foundation (NSF) Graduate Fellowship, and the MIT Karl Taylor Compton Fellowship. In 2006, she was selected as one of the five national recipients of the L'Oréal For Women in Science Postdoctoral Fellowship.